Water Practice & Technology

IWA PUBLISHING

Water Practice & Technology Vol 18 No 4, 947 doi: 10.2166/wpt.2023.042

Synthesis of activated carbon from banana peels for dye removal of an aqueous solution in textile industries: optimization, kinetics, and isotherm aspects

Talbachew Tadesse Nadew [a,*], Mestawot Keana[b], Tsegaye Sisay[c], Belay Getye[c] and Nigus Gabbiye Habtu[d]

[a] Department of Chemical Engineering, College of Chemical and Food Engineering, Wollo University, Kombolcha Institute of Technology, Kombolcha, Ethiopia
[b] Faculty of Chemical and Food Engineering, Bahir Dar Institute of Technology, Bahir Dar University, Bahir Dar, Ethiopia
[c] Department of Chemical Engineering, College of Biological and Chemical Engineering, Addis Ababa Science and Technology University, Addis Ababa, Ethiopia
[d] Bahir Dar Institute of Technology, Bahir Dar University, Ethiopia
*Corresponding author. E-mail: talewtadesse4897@gmail.com; talewtadesse1947@gmail

TTN, 0000-0003-3530-6993

ABSTRACT

Treatment of harmful chemicals using materials at our disposal is the way forward. This study activated bio-adsorbent from waste banana for dye removal from an aqueous solution. The banana peel was activated both thermally and chemically with a preliminary study of a 0.5–2.5 M sulfuric acid concentration, and 50–90 °C of temperature for 1–5 h activation time. Activation at 1.5 M acid concentration, 70 °C for 3 h showed a promising efficacy of about 90% of removing dye. Activated banana peel was characterized using proximate analysis, BET, TGA, SEM, XRD, and FTIR. BET results showed activated banana peel to be porous material with a surface area of 432 m2/g. The adsorption capacity of the adsorbent with different variables range (adsorption time 20–140 min, pH 1.0–7.0, adsorbent dose 1–4 g/L and initial dye concentration 20–80 mg/L) was tested based on a preliminary study. The adsorption process was optimized numerically and the results were; adsorption time 60 min, pH 3, adsorbent dose 2 g/L and initial dye concentration 40 mg/L. The pseudo-second-order kinetics model and Langmuir isotherm model were the best fit to describe the adsorption process.

Key words: activated carbon, adsorption, banana peel, dye, optimization

HIGHLIGHTS

- Adsorption of reactive blue dye using activated banana peel.
- Optimum conditions for adsorption are 60 min adsorption time, 3 pH, 2 g/L adsorbent dose and 40 mg/L initial dye concentration.
- Activated bio-adsorbent from banana peel has 432 m^2/g surface area.

GRAPHICAL ABSTRACT

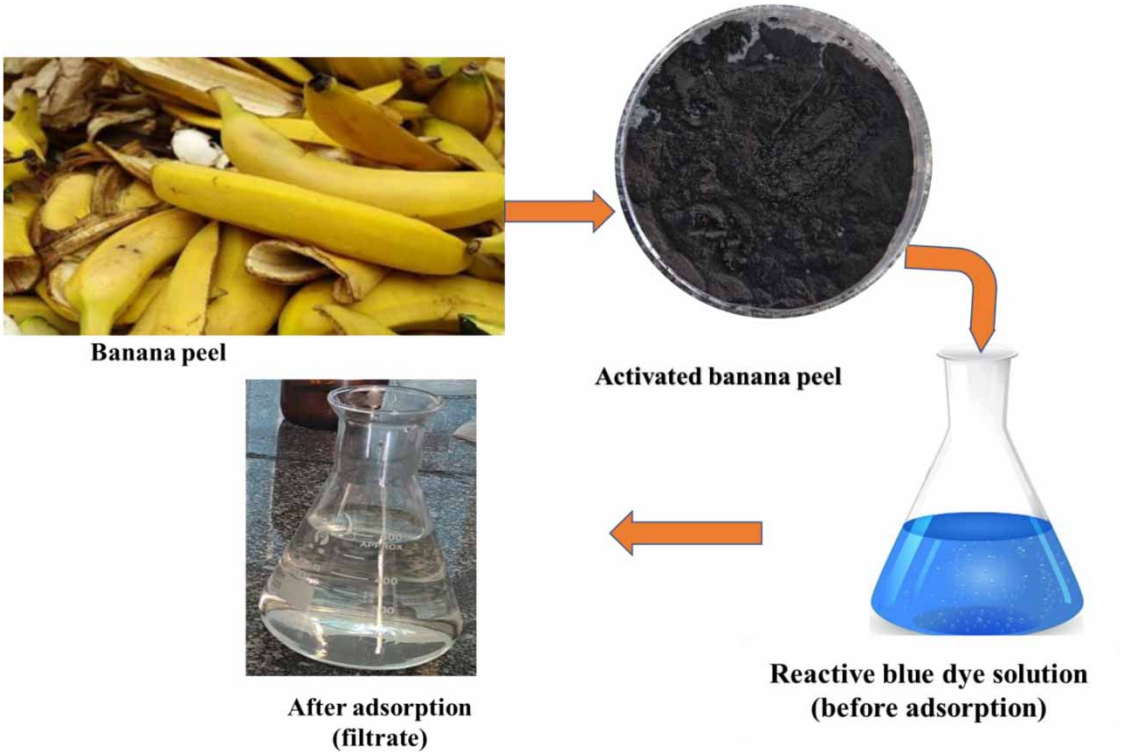

1. INTRODUCTION

Environmental degradation has become worse in recent years as a result of the release of numerous industrial effluents. Untreated solid and liquid sewage is recklessly discharged in large quantities into rivers and streams, particularly those that run through cities, towns and various production areas (Koyachew 2016). As a result, the water body has become heavily contaminated with several pollutants. Moreover, pollution raises the price of water purification and reduces the volume of available water. Thus, it is advocated that all wastewater types that are most likely to be released into the environment be treated to prevent pollution (Afrad *et al.* 2020).

Major water contaminants include a variety of organic and inorganic substances such as heavy metals and industrial compounds. They have the potential to harm human health and obstruct industrial or agricultural water use (Akpor & Muchie 2011). When the level of a pollutant in the water supply exceeds an acceptable threshold for certain water usage, such as drinking or industrial water supply, the water is termed unsafe (Sharma & Bhattacharya 2017; Bodini *et al.* 2021).

Dyes are organic pollutants that are made up of synthetic aromatic organic chemicals that bind to textiles or surfaces to give them color. Synthetic dyes are common water contaminants due to their high solubility, and they are frequently detected in trace amounts in industrial wastewater (Ziarani *et al.* 2018). Industries such as textile, cosmetics, food and paper sectors utilize dyes. However, if dyes are not properly disposed of after usage in these sectors, they can be harmful to the environment (Sarkar *et al.* 2017). Dyes may have a major impact on photosynthetic activity in aquatic life because of the presence of aromatic metals, chloride and other chemicals. One of the most problematic aspects of dye treatment is that the majority of dyes used in industry are resistant to light, oxidation and aerobic digestion. Dyes, on the other hand, are typically synthetic and have a complex aromatic molecular structure that makes them more stable, making them non-biodegradable (Chen & Zhao 2009). Because of their high chemical and biological oxygen demands, suspended particles, turbidity and hazardous components, dyes in wastewater undergo biological and chemical transformations, which deplete dissolved oxygen (Singh & Arora 2011).

Chemical-based textile dyes, in contrast to natural dyes, have become increasingly popular in the textile and dyeing sectors due to their cost-effectiveness and great stability toward many parameters such as high temperature and light. As a result, extremely contaminated effluents are discharged from those sectors (Bhatia *et al.* 2017).

The color and organic content of wastewater from textile dyeing and finishing activities are often high. The effluent from the textile sector is known to be brightly colored, contains a significant number of suspended particulates, has a wide pH range, is hot and has a high chemical oxygen demand (Saini 2017). If dyes are left untreated, they can survive in the aquatic environment for a long time due to their great thermal and light stability. Water-soluble textile dyes have had a significant impact on the fragile ecosystems surrounding industries, and they pose serious environmental issues. A relatively little amount of dye in water is extremely visible and limits light penetration in water systems, causing photosynthesis to suffer (Carmen & Daniela 2010; Gulnaz *et al.* 2011).

The reason for this is that dyes are generally colored and so can tint surface water. It is well acknowledged that the color of water has a significant impact on the public impression of its quality. Color is the first contaminant to be detected in wastewater. Water with very small quantities of colors (less than 1 ppm for some colors) is very visible and unpleasant (Ardila-Leal *et al.* 2021).

Chemical and physical treatment methods for dyes in effluent include adsorption, coagulation, precipitation, filtration, membrane separation and oxidation. Dye-containing wastewaters are difficult to treat because the dyes are refractory molecules (especially azo dyes), resistant to aerobic digestion, durable to oxidizing agents and may be present in small amounts. Traditional color removal processes may be cost-prohibitive and/or technically challenging (Chatzisymeon *et al.* 2006; Nahiun 2021). As a result, an effective treatment of wastewater containing dyes is required. Chemical reduction, ion exchange, evaporation, reverse osmosis and chemical precipitation are some of the methods for treating wastewater containing colors. The drawbacks of utilizing these approaches include the high capital and operating costs, as well as the disposal of leftover sludge (Kumar *et al.* 2012). The bio-adsorption technique with optimum conditions is an appealing option for treating contaminated water, especially if the adsorbent is affordable and does not require any extra processing prior to use. There are a number of articles and review papers researched before year to year. Reviewing different articles in the literature, four parameters considered to affect the adsorption processes mostly were found to be adsorption time, pH, adsorbent dose and initial dye concentration. However, optimization of the adsorption process variables and studying the adsorption mechanism should be adapted to reduce labor and costs. This study aimed to synthesize and determine the banana peel's adsorptive capacity for removing reactive dye (reactive blue) and to investigate the adsorption process and effect of operating parameters such as adsorption time, pH, adsorbent dose and initial dye concentration on the removal of reactive dye from aqueous solutions. Banana peel is a waste product that can be found in great quantities. In addition to treating the dye effluent, converting scrap banana peel into usable bio-adsorbent reduces the amount of home garbage.

2. MATERIALS AND METHODS

2.1. Materials and chemicals

The material used in this study was the banana peel to prepare an activated banana peel bio-adsorbent. The reactive blue dye was chosen as a model pollutant (adsorbate) obtained from Bahir Dar textile industry wastewater. Chemicals (H_2SO_4, HCl, NaOH all with 99% purity) were used to activate the banana peel adsorbent and to adjust the desired level of pH during the experiments.

2.2. Methods

2.2.1. Sample preparation

The raw banana peel was collected from a local juice house in Bahir Dar, Ethiopia. The banana peel was washed with distilled water to remove the remaining dust materials. The size of the peel was reduced from 1 to 2 cm to accelerate the drying process. After all the dripping water was sun-dried, the peel was placed in an oven (Cooper technology, TD-1315/v/c, 2016) for 24 h at 105 °C to remove the moisture content. The dried peel was powdered using an attrition mill. The powdered banana peel was sieved (IC-205/EV) and the particle size below 125 μm was retained. It was then weighed and packed in an air-tight plastic bag.

2.2.2. Synthesis of activated banana peel bio-adsorbent

A two-stage activation process was conducted; a physical activation succeeded by a chemical action. These two action methods would result in an enhanced porosity and hence produce an activated banana peel bio-adsorbent with a relatively large surface area. The physical activation particularly was a thermal treatment to vent out volatile components that leave vacant space on the precursor (banana peel) (Jjagwe *et al.* 2021). For this process, 20 g

of the sample was subjected to 350 °C at a rate of 10 °C/min for 3 h in a furnace under an N_2 environment, based on the method adopted by Zamora-Ledezma *et al.* (2021). After being cooled and size reduced to 125 μm, the sample was further activated chemically at different operating conditions. The bio-adsorbent passed a subsequent physical (under 350 °C temperature and inert environment) and acid activation with variation in acid concentration, temperature and activation time. Acid activation is one of the most common chemical treatments and has been used to increase the specific surface area and the number of acidic centers, modify the surface functional group and obtain solids with high porosity (Kumar *et al.* 2013; Shuma *et al.* 2019). The parameters considered for the activation process are acid (sulfuric acid) concentration, activation temperature and activation time (Table 1). These parameters were studied in a range of different levels to scrutinize the respective effect and to see at which operating conditions can the bio-adsorbent best be synthesized.

Table 1 | Parameter ranges of acid activation of banana peel bio-adsorbent

Varying parameter	Range of parameter					Fixed parameter
Acid concentration (M)	0.5	1.0	1.5	2.0	2.5	At 70 °C and 3 h
Temperature (°C)	50	60	70	80	90	At 1.5 M and 3 h
Time (h)	1	2	3	4	5	At 70 °C and 1.5 M

2.2.3. Physicochemical characterization of adsorbent (activated banana peels)

Proximate analysis: the proximate studies (moisture content, volatile matter, fixed carbon and ash content all in percent) of the activated banana peel were determined using ASTM standard procedures as used in many studies (Shuma *et al.* 2019; Kassahun *et al.* 2022).

pH of point of zero charge determination: Point zero charge is when the net charge on the adsorbent surface is zero (Saruchi & Kumar 2019). The surface charge of the adsorbent depends on the pH of the solution and its pH of point zero charges, pH_{pzc} (Liu *et al.* 2010; Bakatula *et al.* 2018). The adsorbent surface will be negatively charged when $pH > pH_{pzc}$ and positively charged if the $pH < pH_{pzc}$ (Belachew & Hinsene 2020). A 1.5-g of adsorbent was added to 45 mL of 0.1 N KNO_3 solution in the pH range of 2–14. The pH solution was adjusted by adding drops of 0.1 N NaOH and HCl solutions. Each flask was sealed and shaken thoroughly for 48 h at room temperature. Finally, the pH was measured and recorded. The net charge (ΔpH) on acid- and base-activated banana peel surfaces was determined by the difference between initial pH and pH after 48 h.

Scanning electron microscopy (SEM): the morphology of a synthesized activated banana peel bio-adsorbent was studied by plating the activated banana peel on an aluminum stub coated with carbon conductivity tape sample holder and put into SEM (FEI, INSPCT-F50, Germany). The operating conditions used to observe the SEM image were 20 kV, 16 mm working distance, more than 5,000*x* magnification, 20 μm scale and vacuum pressure (Birhanu *et al.* 2020).

Brunauer–Emmett–Teller (BET) surface area analyzer: A 0.4 g of sample was weighed and added into the preparation unit of the surface analyzer (Horiba 96000 series) where the sample was subjected to a temperature of 150 °C for 2 h to remove (degas) the moisture content. The methods and procedures employed for measuring BET surface area were followed and adopted by many authors (Naderi 2015). Based on the single nitrogen molecule surface area and the nitrogen adsorbed–desorbed of the multipoint data, the surface area of the sample was determined.

Fourier-transform infrared spectroscopy (FTIR): Functional groups of an activated banana peel bio-adsorbent were analyzed using FTIR (Thermo Scientific iS50 ABX) instrument equipped with ATR (attenuated total reflection) accessory, Potassium bromide (KBr) beam splitter and detector. After the background was taken, the samples were placed on the sample holder and an IR light source was applied to collect data at 32 resolution and 16 scans. The infrared solution was analyzed in the range of 4,000 and 400 cm^{-1} wavenumber (Turki *et al.* 2018).

Thermal gravimetric analyses (TGAs)*:* 20 g of an activated banana peel bio-adsorbent sample was weighed and placed into a ceramic sample holder separately. The samples were then put into a temperature-controlled TGA cell (DTG-60H) and were set to decompose from ambient temperature to 800 °C. The percentage of mass loss as function temperature was recorded and analyzed (Saadatkhah *et al.* 2020).

2.2.4. Batch adsorption experimental and optimization of adsorption processes

Batch adsorption experiments: this was carried out to achieve the optimum operating conditions for the removal of the selected dye from the aqueous solution (Banerjee *et al.* 2013). A reactive blue dye 19 (**$C_{22}H_{16}N_2Na_2O_{11}S_3$, 99% pure**) solution with a concentration of 1,000 mg/L was prepared as a stock solution. To know the maximum wavelength absorbency of reactive blue dye, 25 mg/L of the dye solution was taken and scanned using a UV–Vis spectrophotometer (DR 5000). The maximum wavelength (λ-max) and absorbance of the dye were taken and scanned from 300 to 700 nm using a UV/VIS spectrometer and it was found at 660 nm. Also, a series of batch experiments were made by diluting this solution. Reactive blue dye solutions with concentrations ranging from 0 to 100 mg/L were prepared by dilution of the stock solution.

A 0.1 M of NaOH and HCl solutions were used to adjust the pH of the adsorption process as was the case required. A cylindrical flask was used to allow the adsorption process at a fixed mechanical stirring of 300 rpm. The filtrate was filtered through Whatman filter paper and analyzed for residual concentration. The response (removal efficiency) was determined using Equation (1). The concentrations of dye after the adsorption process were determined by UV-spectroscopy. The filtrate from each experiment was analyzed using UV-spectrometer and the residual concentrations were read against calibrated values (Harsha Hebbar *et al.* 2018).

$$R\ (\%) = \frac{(C_0 - C_f)}{C_0} * 100 \tag{1}$$

where R is the percentage removal (amount adsorbed) in %, C_0 is the initial dye concentration, mg/L and C_f is the final dye concentration, mg/L.

The optimization and interaction effects of the variables on the adsorption processes were studied using response surface methodology followed by central composite design (RSM-CCD).

Individual parameter effect: The influence of each parameter on the dye adsorption uptake capacity of an acid-activated banana peel bio-adsorbent was studied based on one variable at a time approach. Therefore, adsorption time ranging from 20 to 140 min, pH from 1 to 7, the adsorbent dose from 1.0 to 4.0 g/L, and initial dye concentration from 20 to 80 mg/L have been considered. The parameters considered along the level studied are shown in Table 2.

Table 2 | Parameters and levels to study individual effects

Factors	Unit	Level						
Adsorption time	min	20	40	60	80	100	120	140
pH	–	1.0	2.0	3.0	4.0	5.0	6.0	7
Adsorbent dose	g/L	1.0	1.5	2.0	2.5	3.0	3.5	4.0
Initial concentration	mg/L	20	30	40	50	60	70	80

Interaction effects and model evaluation using RSM-CCD: To investigate the adsorption process other than individual effects, consideration of the interactive effect of parameters on the process makes logical sense. The interaction effect and optimization of parameters were performed using RSM. The levels of each parameter for this study are given in Table 3.

Table 3 | Adsorption factors and corresponding levels for RSM-CCD experiments

			Level	
Factors	Factor symbol	Unit	Lower	Upper
Adsorption time	A	min	40	80
pH	B	–	2	4
Adsorbent dose	C	g/L	1.5	2.5
Initial concentration	D	mg/L	30	50

The RSM-CCD in Design Expert® software version 12.0 produced a total of 30 experiments based on the empirical equation $2^n + 2n + c$. where c is the number of center point experiments and 'n' is the number of independent parameters (Sadhukhan *et al.* 2016; Guo *et al.* 2021). Response surface regression for the design response was analyzed by a quadratic model given by Equation (2) (Behboudi-Jobbehdar *et al.* 2013).

$$Y = \beta + \alpha_1 X_1 + \alpha_2 X_2 + \alpha_3 X_3 + \alpha_4 X_4 + b_1 X_1 X_2 + b_2 X_1 X_3 + b_3 X_1 X_4 + b_4 X_2 X_3 + b_5 X_2 X_4 + b_6 X_3 X_4 + c_1 X_1^2 + c_2 X_2^2 + c_3 X_3^2 + c_4 X_4^2 + \xi \quad (2)$$

where Y is the response variable, β is the intercept constant, α_1–α_4 are main linear effects constant, b_1–b_4 are linear–linear coefficients, and c_1–c_4 are main quadratic effect coefficients, ξ is the error and X_1–X_4 are the independent variables.

2.3. Adsorption kinetics and isotherm studies

2.3.1. Adsorption kinetics

The rate at which the adsorbate (dye) was adsorbed on the surface of the adsorbent (activated banana peel) was studied using well-known kinetics models, namely pseudo-first-order and second-order kinetic models. These kinetics models show the efficacy of the adsorbent, indicating how fast or low it adsorbs the adsorbate. Kinetics is the dynamic of the adsorption process that describes the rate at which the adsorbent adsorbs the dye molecules (Saruchi & Kumar 2019; Shobier *et al.* 2020). To investigate the adsorption of dye on the adsorbent surface, 2 g/L of sample was added to 500 mL of dye solution with an initial concentration of 40 mg/L and pH of 3.0 in a 1,000-mL flask. The solution was stirred at 300 rpm using a mechanical stirrer at room temperature. The adsorption process was examined at adsorption time of 10–160 min. Each filtrate from the adsorption was analyzed for trace concentration of dye. The dye concentration that remained after adsorption in the given time interval was determined using spectroscopy at a wavelength of 660 nm (Khosravi *et al.* 2018; Bai *et al.* 2020; Shobier *et al.* 2020). The amount of dye adsorbed with respect to time (q_t) was calculated using Equation (3) (Zhang *et al.* 2020). The kinetics data of the dye on the surface of the activated banana peel bio-adsorbent samples were fitted to pseudo-first-order and pseudo-second-order kinetics models and the best fit was selected based on the higher value of R^2 (Afolabi *et al.* 2020; Han *et al.* 2020).

$$q_t = \frac{(C_0 - C_t)}{m} * V \quad (3)$$

where q_t is the amount of adsorbate adsorbed at time t, mg/g, C_0 and C_t are the initial concentration and the concentration of dye at time t in mg/L, respectively, V is the volume of the dye solution, L and m is the mass of the adsorbent, g.

Similarly, the amount of adsorbate at equilibrium (q_e) was calculated using Equation (4)

$$q_e = \frac{(C_0 - C_e) * V}{m} \quad (4)$$

where C_e is the dye concentration at equilibrium in mg/L. For the 2 g/L of mass adsorbent used, pH of 3.0 and dye concentration of 40 mg/L, to get an equilibrium concentration 4 h was used to guarantee equilibrium attained where the concentration no longer varies thereafter. The pseudo-first-order kinetics model is given by Equation (5).

$$\frac{dq_t}{d_t} = K_1(q_e - q_t) \quad (5)$$

where q_e is the adsorption capacity at equilibrium, mg/L, K_1 is the pseudo-first-order rate constant, min^{-1} and t is the adsorption time in min. Integration of Equation (5) and taking boundary conditions of $t = 0$ to $t = t$ and $qt = 0$ to $qt = qt$, the pseudo-first-order kinetics are then given by Equation (6).

$$\log(q_e - q_t) = \log(q_e) - \frac{K_1}{2.303} t \quad (6)$$

The pseudo-second-order kinetics model similarly is expressed as Equation (7) and when integrated it is Equation (8).

$$\frac{dq_t}{d_t} = K_2(q_e - q_t)^2 \tag{7}$$

$$\frac{1}{(q_e - q_t)} = \frac{1}{q_e} + K_2 t \tag{8}$$

Where K_2 is the pseudo-second-order adsorption rate constant, g(mg)$^{-1}$min^{-1}.

2.3.2. Adsorption isotherm

Isotherm models show the equilibrium amount of adsorbate available in the solution and the amount of adsorbate available on the surface of adsorbent. Langmuir and Freundlich are the most robust models used to mathematically predict equilibrium adsorption processes. Adsorption isotherm experiments were conducted by adding 2 g/L of adsorbent to 500 mL of different initial concentrations of 25, 45, 65, 85, 105 and 125 mg/L of the adsorbate to be adsorbed, with pH of 3.0 and the adsorption process was agitated by a mechanical stirrer for 4 h of time. After each adsorption was finished, the adsorbent was filtered, the equilibrium concentrations were determined using UV-spectroscopy and the corresponding amount of adsorbate at equilibrium (q_e) was calculated.

The linear form of the Langmuir isotherm model is given as Equation (9).

$$\frac{C_e}{q_e} = \frac{1}{q_{\max} K_L} + \frac{C_e}{q_{\max}} \tag{9}$$

where C_e is the adsorbate concentration at equilibrium in mL/L, q_e is the amount of sorbate at equilibrium per unit mass of sorbent in mg/g, $q_{\max}$ is the complete monolayer sorption capacity at equilibrium in mg/g and K_L is the Langmuir equilibrium constant in L/mg. The experimental data were linearly regressed as C_e/q_e versus C_e, from which the Langmuir constants $q_{\max}$ and K_L were determined from the slope and intercept, respectively. Moreover, the experimental data were also fitted to the Freundlich isotherm model which is expressed by Equation (10).

$$\ln(q_e) = \left(\frac{1}{n}\right) \ln(C_e) + \ln(K_F) \tag{10}$$

where K_F is the Freundlich constant related to adsorption capacity, and n is the Freundlich constant related to adsorption intensity. The Freundlich constants were determined using the straight-line plot of $\ln(q_e)$ versus $\ln(C_e)$ from which n was found from the slope and K_F from the intercept.

2.4. Reusability test of the activated banana peel bio-adsorbent

Several adsorption and desorption processes had been made to test the reusability of the activated banana peel bio-adsorbent over the adsorption of dye molecules (Dahiru *et al.* 2018). A 2 g/L of the adsorbent was allowed to adsorb 40 mg/L of dye molecules at ambient temperature for 4 h and shacked at 500 rpm. The precipitate was added to 500 mL of 0.1 M NaOH solution and shacked for 12 h and then washed several times using distilled water until the pH became neutral. The supernatant solution was analyzed and the removal capacity was determined. The adsorption–desorption process was repeated 10 times until the capacity of the adsorbent fell below 50%.

3. RESULT AND DISCUSSIONS

3.1. Removal efficiency of adsorbent

The activated banana peel bio-adsorbent so produced was allowed to adsorb a solution of dye. The removal efficiency of the bio-adsorbent with respect to sulfuric acid concentration, activation temperature and the activation time is shown in Figure 1(a)–1(c). From Figure 1(a), the removal efficiency increases at a fast rate from 65 to 88% when the acid concentration increases from 0.5 to 1.5 M. A further increment of acid concentration to 2.5 M was found to cause the removal efficiency of the activated banana peel bio-adsorbent to decline to 76%. The result revealed that acid concentration has two-fold implications on the efficiency of the adsorbent. At relatively low

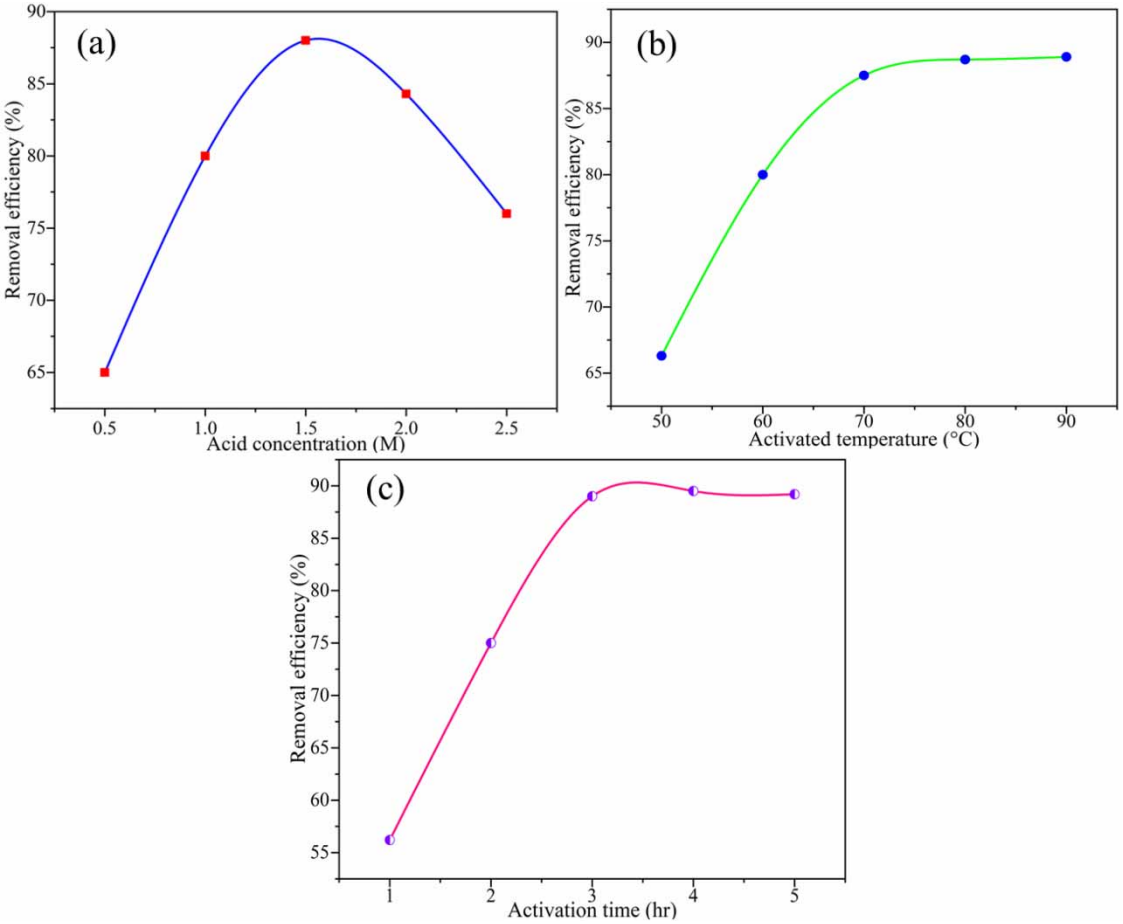

Figure 1 | Removal efficiency of banana peel bio-adsorbent as a function of acid concentration (a), as a function of activation temperature (b), and as a function of activation time (c).

concentrations, the removal efficiency increases which implies the good preparedness of the sample and the availability of more surface area for the accommodation of dye molecules. It seems that after 1.5 M the acid decomposed the amorphous part of the cellulose in the banana peel and causes a porous structure to be developed. The decline of removal efficiency at elevated acid concentration may attribute to the degradation of the main structure and loss of porosity for dye molecules to be adsorbed on. A similar result can be seen in the study by Ali *et al.* (2016) where hydrochloric acid was used to activate banana peel for the removal of hexavalent chromium from an aqueous solution.

As can be seen Figure 1(b), at a fixed acid concentration of 1.5 M and 3 h of activation time, the removal efficiency of the adsorbent increased with the activation temperature. In a similar pattern, the removal efficiency of the adsorbent as a function of activation time at an acid concentration of 1.5 M and at an activation temperature of 70 °C is depicted in Figure 1(c). It increased rapidly from 56.2 to 89% when the activation time changed from 1 to 3 h. However, the efficiency does not change substantially despite the time increasing to 5 h. As illustrated in the graph, an activation time of 3 h seems an ideal operating condition along the optimum acid concentration and activation temperature. As a result, it appears on the surface that acid concentration of 1.5 M, activation temperature of 70 °C and activation time of 3 h are favorable conditions to get an activated banana peel that fulfills the requirements of the adsorbent.

3.2. Characteristics of an activated banana peel bio-adsorbent

3.2.1. Proximate analyses

The moisture content, volatile matter, ash and fixed carbon content of the raw banana peels and activated banana peel bio-adsorbent are shown in Table 4. The parameters of the bio-adsorbent improved owing to the preparation and activation processes as compared to the raw banana peel. According to the study by Hammouda & Mihoubi

Table 4 | Proximate analyses

S/N	Parameter	Result (%)	
		Raw	Activated
1	Moisture content	9.8	4.5
2	Volatile content	19.1	17.7
3	Ash content	6.4	5.2
4	Fixed carbon	64.7	72.6

and Kramarenko *et al.*, the moisture content of the prepared raw banana peel is between 7 and 10% and that of activated is about 5–7% (Hammouda & Mihoubi 2014; Kramarenko *et al.* 2016).

3.2.2. Point of zero charge (pH_{pzc}) analysis

A plot of final pH values against the initial pH value (pH_i) is presented in Figure 2. From the plotted curve, the significance of these pH values is that a given adsorbent surface will have a positive charge at solution pH values less than the pH_{pzc} and thus can be used to absorb anion adsorbates. On the other hand, the surface has a negative charge at a solution pH value greater than the pH_{pzc} and is suitable to adsorb cations on its surface. The pH_{pzc} is identified and seen that the pH_{pzc} of the banana peel surface was found to be 4.67. At pH less than 4.67, the bio-sorbent is positively charged because H^+ ions reside on the surface. At pH greater than 4.67, the bio-sorbent is negatively charged because H^+ ions enter a high-pH solution, resulting in a negatively charged (H^+ poor) surface. An approximated result was reported for the adsorption of ionic reactive dyes over Alfa powder from the leaf of *Stippa tenacissim* at a lower pH value and that adsorption capacity increased with decreasing pH of the solution (Palma *et al.* 2011).

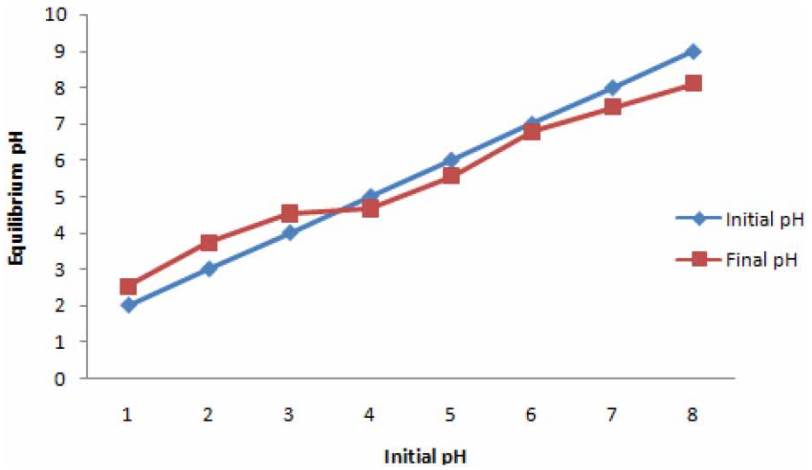

Figure 2 | Point zero charge (pH_{pzc}) of activated banana peel bio-adsorbent.

3.2.3. SEM analysis

The morphology of raw banana peel and activated banana peel bio-adsorbent was analyzed with SEM and the image is depicted in Figure 3(a) and 3(b). It unveiled the distinction of the images in terms of porosity and surface morphologies. Due to preparations and activation processes, the activated banana peel bio-adsorbent appears to have more surface and porosity. A more or less similar result can be seen from the previous study (Ramutshatsha-makhwedzha *et al.* 2022) in which case the activated adsorbent assumed much more surface.

3.2.4. BET analyses

Surface area is a paramount characteristic of adsorbents as the adsorption process is a surface phenomenon. As is the case with all adsorbents, the activated banana peel produced by the physical and chemical processes is

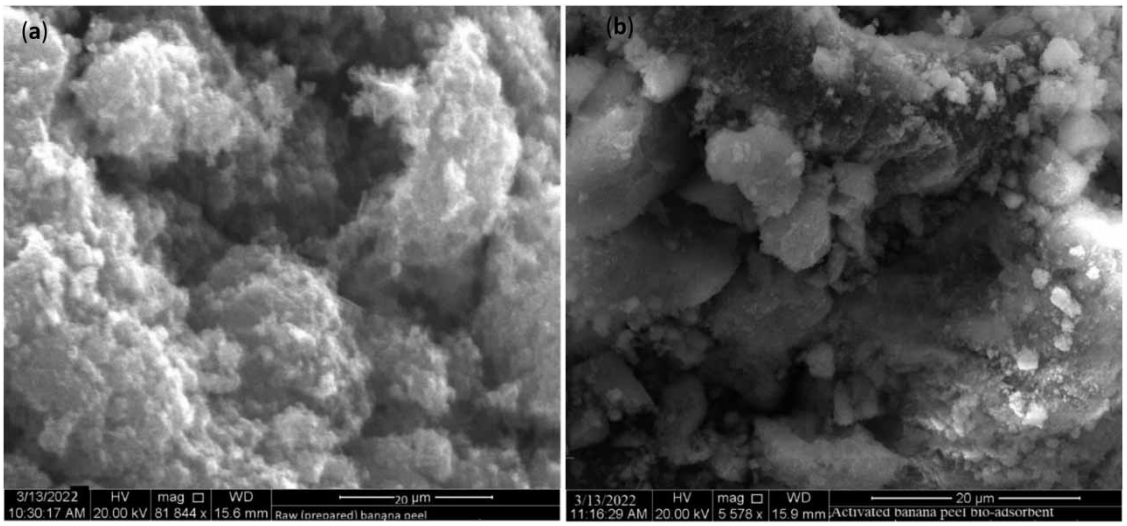

Figure 3 | SEM results of raw banana peel (a) and activated banana peel (b).

assumed to have enough surface to qualify for dye adsorption. The BET results showed that surface areas of the raw banana peel and activated banana peel bio-adsorbent to be 75 and 432 m^2/g, respectively. Sinto *et al.* reported surface area of activated banana peels to be 426 m^2/g using different techniques (Sinto *et al.* 2018).

3.2.5. FTIR analyses

The FTIR spectra of raw and activated banana peels are presented in Figure 4. It can be seen from the spectra that there are some functional groups in both samples at 3,684.94; 3,619.38; 1,117.03; 1,005.01; 912.49; 672.95 and 529.33 wavenumbers (cm^{-1}). The weak peak at 3,684.94 and 3,619.38 wavenumbers (cm^{-1}) may show the existence of moisture content, probably OH group. The peak at 1,117.03 wavenumber (cm^{-1}) may be attributed to the presence of C–O. It can be assumed that it is due to the fluoro compound, specifically the C–F stretching group at the peak 1,005.01. Perhaps, the peaks at 672.95 and 529.33 indicate the presence of halo compounds in the sample. Moreover, the change of peak(s) from strong to weak peak patterns might imply that compounds such as water have been removed completely or partially during the activation process. The two spectra are similar in their pattern and are different in the quantity of the functional groups available. As can be seen from the work of Matei *et al.*, the spectra of the activated banana peel are in line with the spectra of these results (Matei *et al.* 2021).

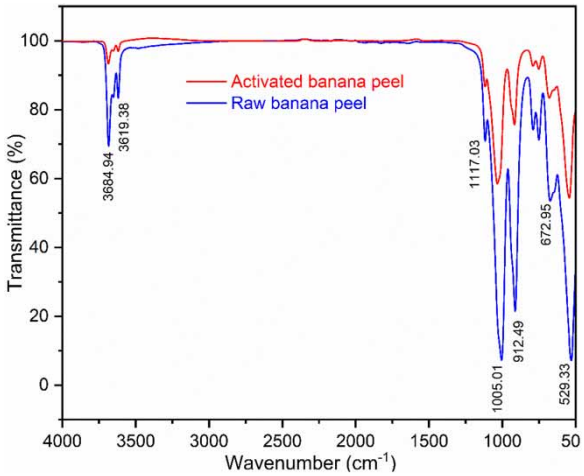

Figure 4 | FTIR spectra of raw and activated banana peels.

3.2.6. TGA of raw banana peel and activated banana peel bio-adsorbent

The TGAs of both raw and activated banana peels have been conducted to analyze the effect of temperature on the sample under oxidized conditions. The result is introduced in Figure 5, the activated banana peel bio-adsorbent started to decompose after 300 °C and the raw sample at 150 °C. The mass loss between 150 and 400 °C might be due to the loss of bounded water and some other impurities. The sharp decline of both curves beyond 400 °C may attribute to the decomposition of the sample into other smaller components such as carbon dioxide.

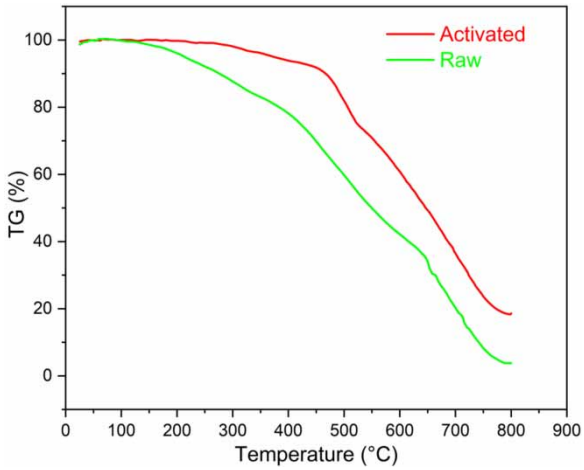

Figure 5 | Percentage of mass loss of raw and activated banana peels with temperature.

3.3. Parameter effects and optimizations

3.3.1. Individual parameter effects on the efficiency of adsorption

The levels of the main adsorption parameters such as adsorption time, pH, adsorbent dose and initial dye concentration were scoped based on the effects they have on the adsorption process following the one-factor-at-a-time method. To scrutinize the adsorption of dye on the surface of the activated banana peel bio-adsorbent, adsorption time in the range of 20–140 min, pH from 1.0 to 7.0, adsorbent dose from 1 to 4 g/L and initial dye concentration from 20 to 80 mg/L were considered and the effect each parameter is plotted in Figure 6(a)–6(d).

Effect of adsorption time: The graph of removal efficiency rapidly increased from 48.6 to 87.6% as the adsorption time varied from 20 to 60 min at a fixed pH of 3, adsorbent dose of 2 g/L and initial dye concentration of 40 mg/L as depicted in Figure 6(a). When the adsorption time further increased to 140 min with the interval shown, the removal efficiency of the bio-adsorbent for dye adsorbate slightly increases and shortly after that tends to remain almost constant at 92%. The increment of removal efficiency as a function of time implies that adsorption requires time to take place. According to Zheng *et al.* (2021) study, the adsorption mass transfer phenomenon involves three main steps: external diffusion, internal diffusion, and attachment to the active site. As a result, it demands a certain period to adsorb a given amount of adsorbate and of course until all the surface available is taken up or equilibrium is attained. Dwivedi *et al.* (2016) discussed 90 min to remove about 84% of cyanide contaminant. The adsorption time sufficient to remove most of the adsorbate may be short or long depending on the type of adsorbent and adsorbate the behavior of adsorption (Deng *et al.* 2014).

Effect of pH: The dyes are complex organic compounds with different functional groups and unsaturated bonds, so they show different levels of ionization at different pHs. In this regard, the biosorption of reactive blue dye solutions was carried out by varying pH of 1–7, with bio-adsorbent dose, initial dye concentration and adsorption time kept constant at 2 g/L, 40 mg/L and 60 min, respectively, and presented in Figure 6(b). The removal capacity of the adsorbent below pH of 3 was found to be around 90% and sharply falls all the way down to 40% as the pH increases to 7. It can be deduced that the solution pH was directly related to the availability of positively charged active sites on the surface of the bio-sorbent to bind with the dye molecules. Since the point zero charge of this particular adsorbent surface is 4.7, it assumes a positively charged surface below a pH of 4.7, as a consequence,

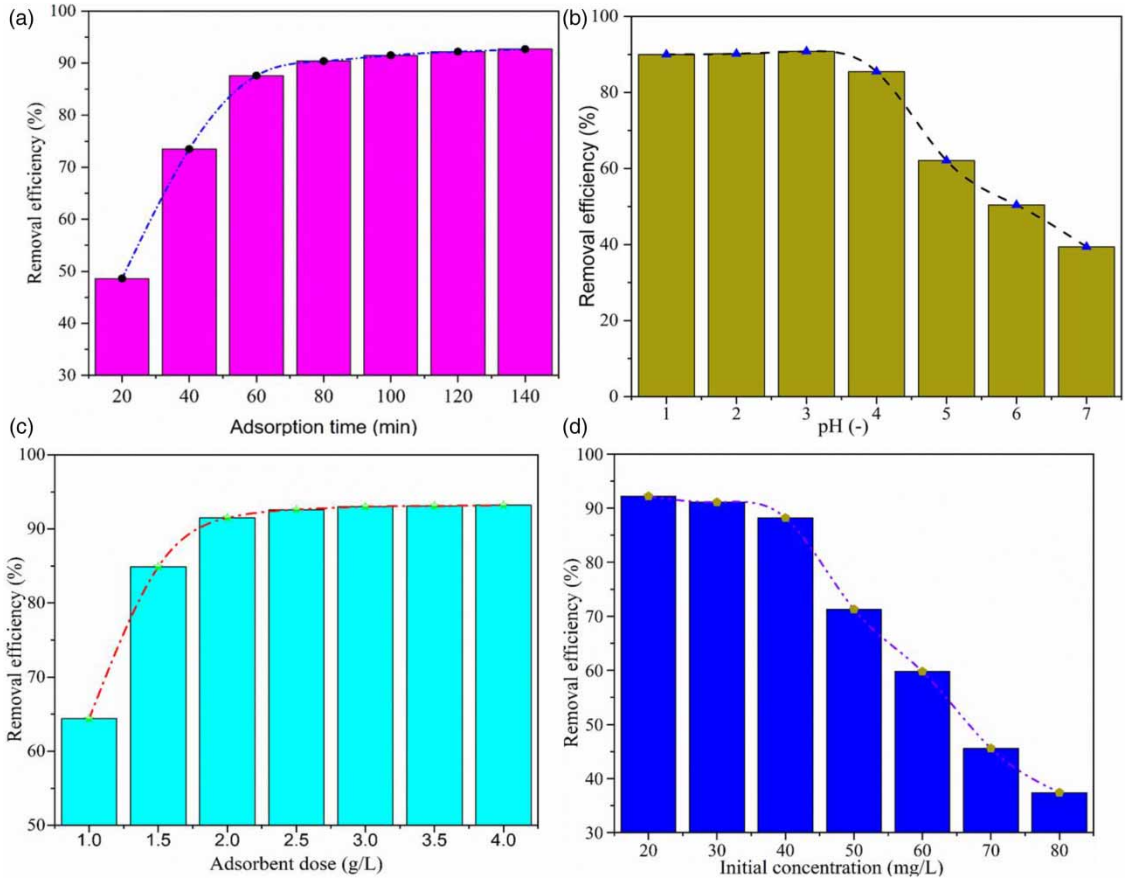

Figure 6 | Effect of adsorption time (a), pH (b), adsorbent dose (c), and dye concentration (d) on percentage of removal efficiency.

adsorption of the anionic dye molecules becomes more favorable at low pH than high ones. The positive ions (H+) provide an electrostatic attraction between the adsorbent surface and the dye molecules leading to maximum adsorption. Some studies reported that the amount of dye uptake decreases with increasing the pH solutions from 2.5 up to 6 (Fernandes *et al.* 2008; Elkady *et al.* 2011; Gulnaz *et al.* 2011).

Effect of adsorbent dose: Adsorbent dose is among the essential parameters that strongly affect the adsorption process as observed in Figure 6(c). The removal efficiency of the adsorbent increases from 64.4 to 91.5% as the adsorbent dose increases from 1 to 2 g/L and appears almost constant thereafter. For a given dye concentration of 40 mg/L, it seems at high doses (say 3 g/L and above) the amount of adsorbate molecules available are already taken and the removal efficiency tends to remain constant.

Effect of initial dye concentration: The removal efficiency of the activated banana peel bio-adsorbent as a function of initial dye concentration of 20–80 mg/L at a fixed adsorption time of 60 min, pH of 3 and adsorbent dose of 2 g/L is demonstrated in Figure 6(d). As can be observed from the graph, the removal efficiency lightly changes from 92.2 to 88.2% as the initial dye concentration varies from 20 to 40 mg/L. when the initial dye concentration increases to 80 mg/L, however, the removal efficiency sharply declines to 37.4%. It is apparent that the dye's initial concentration radically affects the removal efficiency for a given adsorbent of 2 g/L. Increasing the dye concentration (molecules) at this fixed adsorbent amount would mean a small surface area for adsorption.

3.3.2. Interaction effect of adsorption parameters

Analysis of variance (ANOVA) and regression model: In the study, the p^2 and R^2 values are found to be less than 0.0005 and 0.987, respectively. This implies that the quadratic model is best fitted to the experimental data. The feasibility and suitability of the model were analyzed by ANOVA and shown in Table 5. The quadratic equation that predicts the removal efficiency of the activated bio-adsorbent (*RE*%) as a function of adsorption time

Table 5 | Response surface quadratic model of ANOVA for MB removal

Source	Sum of squares	df	Square mean	*F*-value	*P*-value Prob. > F	
Model	6,924.61	14	494.61	82.15	<0.0001	Significant
A	2,527.65	1	2,527.65	419.83	<0.0001	
B	707.42	1	707.42	117.50	<0.0001	
C	216.60	1	216.60	35.98	<0.0001	
D	2,029.52	1	2,029.52	337.10	<0.0001	
AB	14.63	1	14.63	2.43	0.0139	
AC	52.20	1	52.20	8.67	0.0100	
AD	38.75	1	38.75	6.44	0.0228	
BC	16.20	1	16.20	2.69	0.1217	
BD	11.73	1	11.73	1.95	0.1831	
CD	3.71	1	3.71	0.6155	0.4449	
A^2	842.02	1	842.02	139.86	<0.0001	
B^2	348.72	1	348.72	57.92	<0.0001	
C^2	96.75	1	96.75	16.07	0.0011	
D^2	453.38	1	453.38	75.30	<0.0001	
Residual	90.31	15	6.02			
Lack of Fit	90.24	10	9.02	4.24	0.0532	Not significant
Pure error	0.0733	5	0.0147			

(*A*-min), pH (*B*), adsorbent dose(*C*-g/L), and initial dye concentration (*D*-mg/L) is given as Equation (11):

$$RE(\%) = 25.1554 + 0.6339 * A + 13.3566 * B + 88.1102 * C + 0.1560 * D - 0.0016 * AB - 0.0277 * AC + 0.0150 * AD + 2.6460 * BC + 0.2230 * BD + 0.0.3822 * CD - 0.0048 * A^2 - 5.3104 * B^2 - 33.1485 * C^2 - 0.0418 * D^2 \quad (11)$$

The statistical analyses are evident that the actual (experimental) and the model predicted values of the removal efficiencies are alike to an acceptable extent in which case the R^2, adjusted R^2, and predicted R^2 was found to be 0.987, 0.975, and 0.926, respectively. The predicted and actual values of the removal efficiency are plotted in Figure 7.

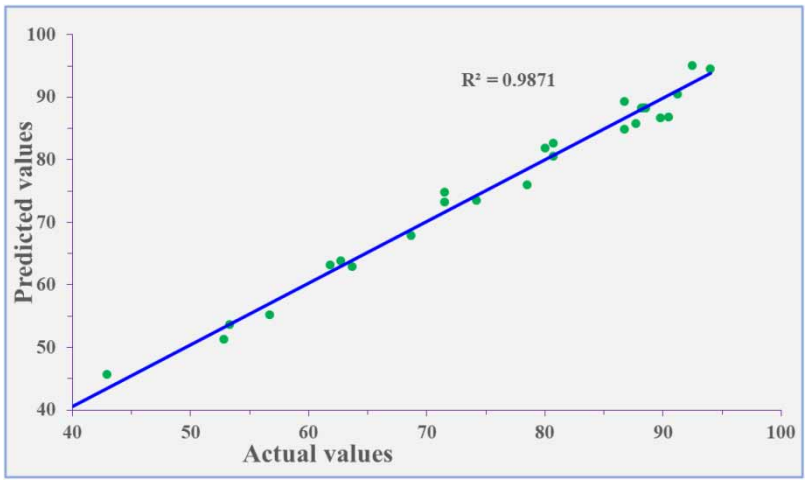

Figure 7 | Actual versus model predicted values fitting.

Interaction effect: The effect of parameters is two-fold; they definitely affect the adsorption process, and one variable affects the others. Parameter interaction is the epicenter of processes that determines the extent to which the processes have a sound result. RSM provides a pair of parameters effect at once in terms of surface plot for easy response visualization. The effects of adsorption time and pH, adsorption time and adsorbent dose, adsorption time and initial dye concentration, pH and adsorbent dose, pH and initial dye concentration, and adsorbent dose and initial dye concentration on the removal efficiency of bio-adsorbent are discussed and presented in Figure 8(a)–8(f), respectively.

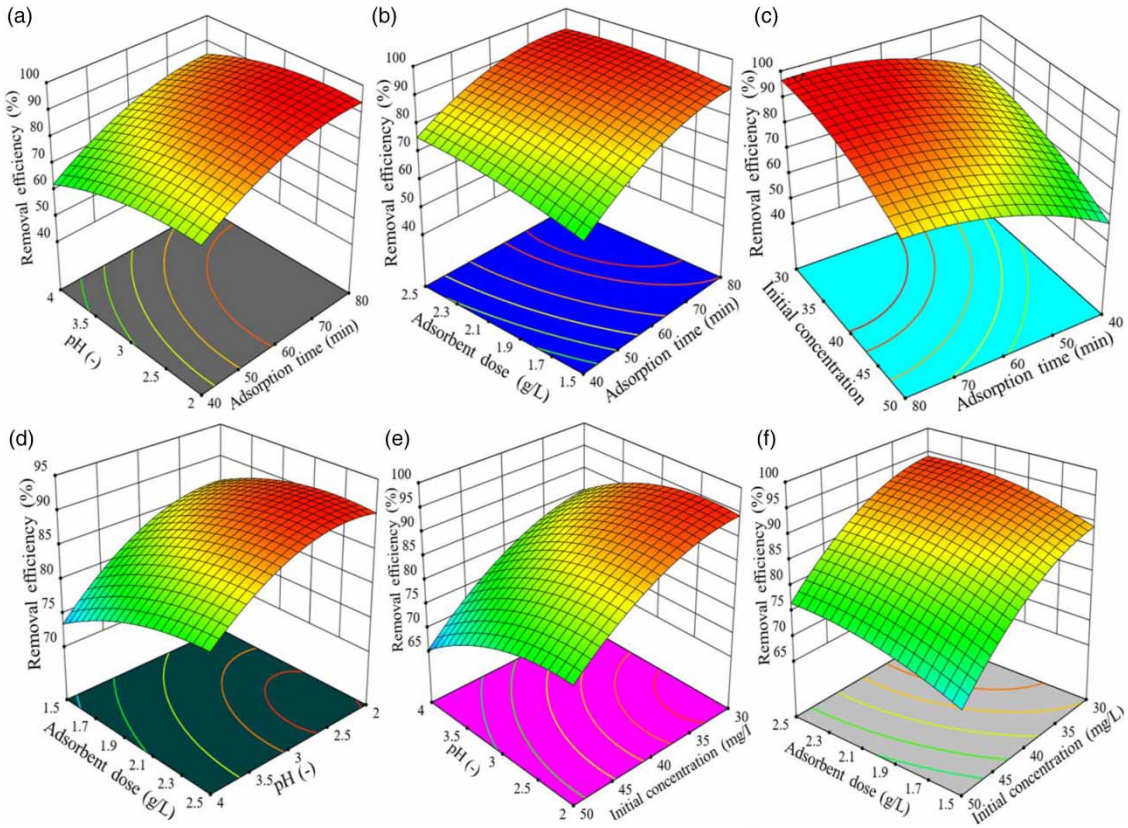

Figure 8 | Interaction effects of parameters on removal efficiency.

The interaction of the effect of adsorption time and pH on the removal efficiency of the bio-adsorbent at a given adsorbent dose of 2 g/L and initial dye concentration of 40 mg/L is illustrated in Figure 8(a). It can be seen from the graph that the removal efficiency rapidly increases from 62.8 to 91.8% as the adsorption time increases from 40 to 66 min and pH decreases from 4 to 2.8. Thereafter, the removal efficiency slowly increases as adsorption time increases to 80 min and pH decreases to 2. The increment of removal efficiency at these given operating conditions may attribute to a favorable condition that the adsorption time and pH conduce for mass transfer to take place rapidly. Moreover, it seems that the activated bio-adsorbent provided relatively enough surface area to adsorb the dye molecules at first and then tends to approach equilibrium where the adsorption process is about to stop. The removal efficiency, thus, was found to be almost constant (Padmavathy *et al.* 2016).

Likewise, Figure 8(b) demonstrates removal efficiency as a function of adsorption time and adsorbent dose at pH of 3 and 40 mg/L of initial dye concentration. It reveals the increment of the removal efficiency from 64.1 to 90.8% when the adsorption time varied from 40 to 64 min and the adsorbent dose varied from 1.5 to 2.1 g/L. Up next, the removal efficiency slightly increases to 92.5% despite the adsorption time and adsorbent dose increases to 80 min and 2.5 g/L, respectively.

The increase in removal efficiency with both adsorbent dose and adsorption time is due to the availability of surface area as the adsorbent amount increases and sufficiently enough time for adsorption (Manoj *et al.* 2015).

Figure 8(c) clearly depicted how the removal efficiency of the activated bio-adsorbent varies with the variation of adsorption time and initial dye concentration at pH 3 and 2 g/L of adsorbent dose. The graph unfolds the increment of the removal efficiency at a considerable rate from 58 to 91.8% when the adsorption time increases from 40 to 64 min and the initial dye concentration decreases from 60 to 38 mg/L. As the model predicted, the removal efficiency shows a slow increase to 96.6% as adsorption time further varied to 80 min and the initial concentration decreased to 30 mg/L. It appears that initial dye concentration played a significant role in the removal efficiency. High efficiency at low concentrations would mean that the activated bio-adsorbent assumed more room for adsorption relative to the molecules of dye. On the other hand, higher dye concentration outnumbers the available surface and causes the removal efficiency to decline sharply (Padmavathy *et al.* 2016).

Figure 8(d) described the surface plots of response removal efficiency of dye adsorption process by the activated bio-adsorbent drawn with the variable's pH and adsorbent dose at a constant adsorption time of 60 min and initial dye concentration of 40 mg/L. It can clearly be observed from the graphs that the removal efficiency of the bio-adsorbent in terms of adsorbing dye molecules has an increment pattern with the adsorbent dose and a decrement pattern with pH. As such, when the adsorbent amount varied from 1.5 to 2 g/L and the pH changed from 4 to 2.8, the efficiency was found to change from 73.8 to 90% at a noticeable rate. It, however, remains constant, give or take, even though the adsorbent increases to 2.5 and pH further decreases to 2. It can thus be concluded that the cumulative effect of both variables to have a sound removal efficiency is in the vicinity of 2 g/L of adsorbent dose and pH of 3 for a given initial dye concentration of 40 mg/L for an adsorption time of 60 min. It also seems that the increase of the adsorbent amount allows more room for the adsorption of dye molecules till the process tends toward equilibrium. At a high-pH dye solution, the adsorption competes with other molecules which causes the efficiency of dye removal to decline rapidly.

The interaction effect of pH and initial concentration on the removal efficiency of the activated bio-adsorbent in the event of dye molecules adsorption is given in Figure 8(e). As would be expected, the removal efficiency is more pronouncedly dependent on the dye concentration for a constant adsorption time of 60 min and an adsorbent dose of 2 g/L. The efficiency was found to go up to 94% when the dye concentration was reduced to 30 mg/L. While the adsorbent amount is kept at 2 g/L, it is crystal clear that the removal efficiency declines with concentration and the reverse holds true. Apparently, since adsorption is a surface phenomenon, higher dye concentration would outnumber the available surface present in the 2 g/L adsorbent and as consequence, some dye molecules remain adsorbed or not removed from the synthetic solution. It is, therefore, imperative that the dye concentration should be proportional to the adsorbent dose which in this case is 2 g/L to 40 mg/L to get about 90% of the dye removed, putting other factors aside.

Figure 8(c) presented the removal efficiency of activated bio-adsorbent concerning adsorbent dose and initial dye concentration at a fixed adsorption time of 60 min and pH of 3. The model equation pretty well predicts the removal efficiency to increase from 70 to 94% based on the variation of adsorbent dose from 1.5 to 2.0 and initial dye concentration from 50 to 30 mg/L. As is so often the case, the removal efficiency tends to increase with the adsorbent dose and decrease with the dye's initial concentration (Al-senani & Al-fawzan 2018). All told, the removal efficiency of activated bio-adsorbent used to adsorb synthetic dye solution was found to be dependent on the four parameters, namely adsorption time, pH, adsorbent dose and initial dye concentration. On top of that, adsorption time and adsorbent dose were found to have a positive effect, and pH and initial dye concentration negative effect on the removal efficiency. It appears on the surface that 90% or so of the dye molecules can be removed at favorable operating conditions of the variables without some extended levels considered (Mohan *et al.* 2006; Padmavathy *et al.* 2016).

Parameter optimization: the indication of the need for optimization that compromises level parameters and yields an acceptable level of removal efficiency. The optimization gives no lower nor higher but in-between values of variables and responses based on the criteria set. The optimum operating conditions of the dye adsorption process were found to be an adsorption time of 60 min, pH of 3, an adsorbent dose of 2 g/L, and an initial dye concentration of 40 mg/L from the RSM-CCD numerical optimization. The optimum operating condition found was validated with triplicated experimental data and the deviation between the experimental result and that of the model predicted was 1.3%.

3.4. Adsorption mechanisms

3.4.1. Adsorption kinetics

The kinetics of dye molecules' adsorption on bio-adsorbent was examined by pseudo-first-order and pseudo-second-order kinetic models. The data obtained were regressed and fitted to pseudo-first-order and pseudo-second-order kinetic models and are shown in Figure 9(a) and 9(b), respectively. The models' fitness with coefficients of determination (R^2) was found to be 0.739 and 0.978, respectively. Comparing the two regressions, the adsorption of dye molecules on the surface of the activated bio-adsorbent prepared from banana peel seems to follow the pseudo-second-order kinetics model.

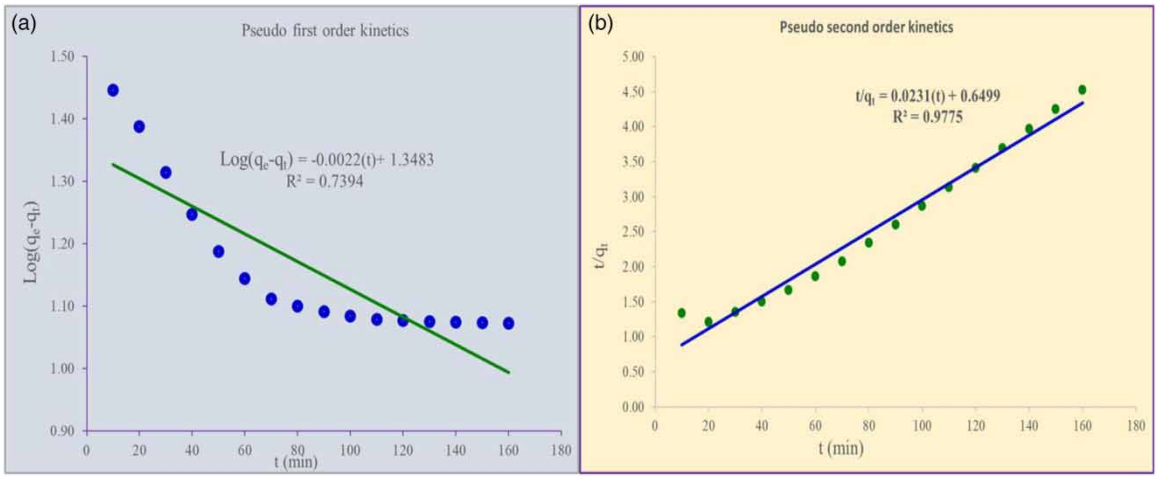

Figure 9 | Pseudo-first-order and pseudo-second-order kinetic data fitting.

3.4.2. Adsorption isotherms

The two well-known isotherm models, Langmuir and Freundlich adsorption isotherm models were used to study the adsorption mechanism. The coefficient of determination (R^2) was used to indicate the isotherm model that best fits with experimental data. The R^2 values and the model parameters or coefficients are presented in Table 6. The adsorption behavior of the dye molecules on bio-adsorbent is best described mathematically using the Langmuir isotherm model since the R^2 value is 0.9996. Furthermore, it can be inferred that the dye molecules formed a monolayer on the surface of the adsorbent.

Table 6 | Summary of adsorption mechanisms

	Pseudo-first-order kinetics			Pseudo-second-order kinetics		
Adsorbent	q_e (mg/g)	K_1 (min^{-1})	R^2	q_e (mg/g)	K_2 ($g(mg)^{-1}min^{-1}$)	R^2
	35.4	0.005	0.7398	35.4	0.0006	0.9775
	Langmuir isotherm parameters			Freundlich isotherm parameters		
Activated banana peel	q_m (mg/g)	K_L (L/mg)	R^2	K_F (mg/g)	n	R^2
	38	0.993	0.9996	24.96	10.11	0.8916

3.5. Reusability of the activated banana peel bio-adsorbent

The performance of the adsorbent with regard to the number of times it can be used to absorb dye molecules is shown in Figure 10. The removal efficiency of adsorbent declined from 93.5% to 48% when it was used at first and for the sixth time following the adsorption–adsorption processes. The potential reuse of activated banana peels is also studied previously by many authors (Pathak *et al.* 2016). It can be concluded that the activated banana peel bio-adsorbent has a good regeneration capacity to use once more.

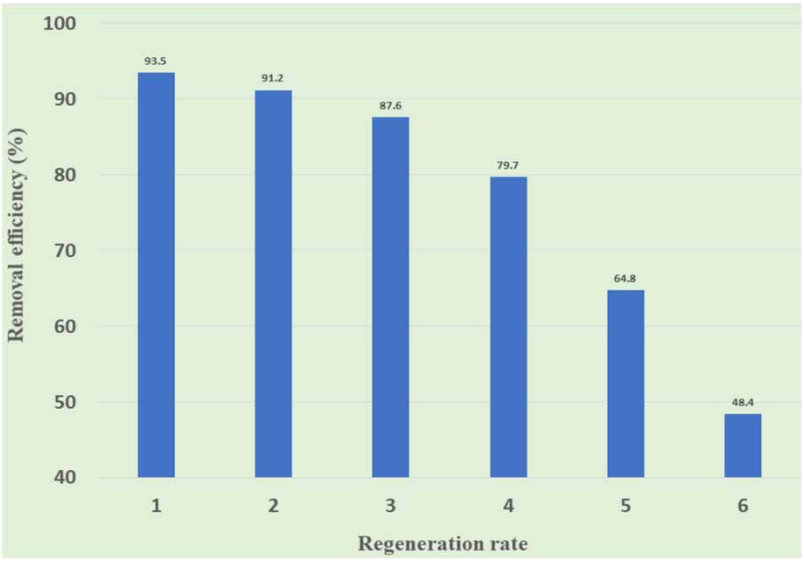

Figure 10 | Regeneration rate of activated banana peel bio-adsorbent.

4. CONCLUSION

This study looked into the bio-adsorption of reactive blue dye onto the activated banana peel. Thermal and chemical surface modifications were done to the bio-adsorbent to boost its ability to absorb the anionic dye, reactive blue. With the surface modification, the change in the surface charges of adsorbent materials was aimed. The characterization methods of the activated banana peel such as proximate analysis, BET, TGA, SEM, XRD, and FTIR gave reliable and guaranteed results for the adsorption of dye from the aqueous solution or textile effluent. The activated banana peel bio-adsorbent was allowed to adsorb the dye molecules at different operating conditions. The operating conditions were optimized and this optimum condition can remove most of the dye molecules from the synthetic solution. From the kinetics and isotherm model study, it can be concluded that the rate at which the dye molecules are being adsorbed and the behavior of adsorption follow pseudo-second-order and Langmuir isotherm models. The regeneration test suggested that the activated banana peel bio-adsorbent can be used four times and repeated before its removal performance falls $<80\%$. To sum it up, activated banana peels can be a good candidate for adsorbent material to mitigate wastewater problems to a considerable extent. Using banana peel as a means to treat wastewater has two-fold advantages: (1) turning a waste material into a useful adsorbent and (2) it is relatively cheap and easy to prepare.

ACKNOWLEDGEMENTS

The authors would like to thank the Department of Chemical Engineering, College of Food and Chemical Engineering, Wollo University, Kombolcha Institute of Technology, Kombolcha, Ethiopia; Bahir Dar University, Bahir Dar, Ethiopia; and Addis Ababa Science Technology University, Addis Ababa, Ethiopia for their collaboration during the laboratory work.

AUTHOR CONTRIBUTIONS

M.K. conceptualized the study, prepared the methodology, did formal analysis, investigated the study, collected resources, and did data curation; T.S. did software analysis, validated the study, wrote and prepared the original draft; B.G. wrote, reviewed and edited the article, T.T. visualized and supervised the study. All authors have read and agreed to the published version of the manuscript.

DATA AVAILABILITY STATEMENT

All relevant data are included in the paper or its Supplementary Information.

CONFLICT OF INTEREST

The authors declare there is no conflict.

REFERENCES

Afolabi, I. C., Popoola, S. I. & Bello, O. S. 2020 Modeling pseudo-second-oOrder kinetics of orange peel-paracetamol adsorption process using artificial neural network. *Chemometrics and Intelligent Laboratory Systems* **203**, 104053. https://doi.org/10.1016/j.chemolab.2020.104053.

Afrad, M. S. I., Monir, M. B., Haque, M. E., Barau, A. A. & Haque, M. M. 2020 Impact of industrial effluent on water, soil and rice production in Bangladesh: a case of Turag River Bank. *Journal of Environmental Health Science and Engineering* **18**(2), 825–834. https://doi.org/10.1007/s40201-020-00506-8.

Akpor, O. B. & Muchie, M. 2011 Environmental and public health implications of wastewater quality. *African Journal of Biotechnology* **10**(13), 2379–2387. https://doi.org/10.5897/AJB10.1797.

Ali, A., Saeed, K. & Mabood, F. 2016 Removal of chromium (VI) from aqueous medium using chemically modified banana peels as efficient low-cost adsorbent. *Alexandria Engineering Journal* **55**(3), 2933–2942. https://doi.org/10.1016/j.aej.2016.05.011.

Al-senani, G. M. & Al-fawzan, F. F. 2018 Adsorption study of heavy metal ions from aqueous solution by nanoparticle of wild herbs. *The Egyptian Journal of Aquatic Research* **44**(3), 187–194. https://doi.org/10.1016/j.ejar.2018.07.006.

Ardila-Leal, L. D., Poutou-Piñales, R. A., Pedroza-Rodríguez, A. M. & Quevedo-Hidalgo, B. E. 2021 A brief history of colour, the environmental impact of synthetic dyes and removal by using laccases. *Molecules* **26**(13). https://doi.org/10.3390/molecules26133813.

Bai, C., Wang, L. & Zhu, Z. 2020 Adsorption of Cr(III) and Pb(II) by graphene oxide/Alginate hydrogel membrane: characterization, adsorption kinetics, isotherm and thermodynamics studies. *International Journal of Biological Macromolecules* **147**, 898–910. https://doi.org/10.1016/j.ijbiomac.2019.09.249.

Bakatula, E. N., Richard, D., Neculita, C. M. & Zagury, G. J. 2018 Determination of point of zero charge of natural organic materials. *Environmental Science and Pollution Research* **25**(8), 7823–7833. https://doi.org/10.1007/s11356-017-1115-7.

Banerjee, D., Sen, D. & Chattopadhyay, K. K. 2013 Microporous and Mesoporous Materials Simple Chemical Synthesis of Porous Carbon Spheres and Its Improved Field Emission by Water Vapor Adsorption. *Microporous and Mesoporous Materials* **171**, 201–7. https://doi.org/10.1016/j.micromeso.2012.12.043.

Behboudi-Jobbehdar, S., Soukoulis, C., Yonekura, L. & Fisk, I. 2013 Optimization of spray-drying process conditions for the production of maximally viable microencapsulated L. Acidophilus NCIMB 701748. *Drying Technology* **31**(11), 1274–1283. https://doi.org/10.1080/07373937.2013.788509.

Belachew, N. & Hinsene, H. 2020 Preparation of cationic surfactant-modified kaolin for enhanced adsorption of hexavalent chromium from aqueous solution. *Applied Water Science* **10**(1), 38. https://doi.org/10.1007/s13201-019-1121-7.

Bhatia, D., Sharma, N. R., Singh, J. & Kanwar, R. S. 2017 Biological methods for textile dye removal from wastewater: a review. *Critical Reviews in Environmental Science and Technology* **47**(19), 1836–1876. https://doi.org/10.1080/10643389.2017.1393263.

Birhanu, Y., Leta, S. & Adam, G. 2020 Removal of chromium from synthetic wastewater by adsorption onto Ethiopian low - cost odaracha adsorbent. *Applied Water Science* **10**(11), 1–11. https://doi.org/10.1007/s13201-020-01310-3.

Bodini, A., Chiussi, S., Donati, M., Bellassen, V., Török, Á., Dries, L., C´orić, D. S., Gauvrit, L., Tsakiridou, E., Majewski, E., Ristic, B., Stojanovic, Z., Roig, J. M. G., Lilavanichakul, A., An, N. Q. & Arfini, F. 2021 Water footprint of food quality schemes. *Journal of Agricultural and Food Industrial Organization* **19**(2), 145–160. https://doi.org/10.1515/jafio-2019-0045.

Carmen, Z. & Daniela, S. 2010 Characteristics, polluting effects and separation/elimination procedures from industrial effluents – a critical overview. *Textile Organic Dye* **472**, 55–86.

Chatzisymeon, E., Xekoukoulotakis, N. P., Coz, A., Kalogerakis, N. & Mantzavinos, D. 2006 Electrochemical treatment of textile dyes and dyehouse effluents. *Journal of Hazardous Materials* **137**(2), 998–1007. https://doi.org/10.1016/j.jhazmat.2006.03.032.

Chen, H. & Zhao, J. 2009 Adsorption study for removal of Congo Red anionic dye using Organo-Attapulgite. *Adsorption* **15**(4), 381–389. https://doi.org/10.1007/s10450-009-9155-z.

Dahiru, M., Zango, Z. U. & Haruna, M. A. 2018 Cationic dyes removal using low-cost banana peel biosorbent. *American Journal of Materials Science* **8**(2), 32–38. https://doi.org/10.5923/j.materials.20180802.02.

Deng, L., Shi, Z., Luo, L., Chen, S.-y., Yang, L.-f., Yang, X.-z. & Liu, L.-s. 2014 Adsorption of hexavalent chromium onto kaolin clay based adsorbent. *Journal of Central South University* **21**(10), 3918–3926. https://doi.org/10.1007/s11771-014-2379-4.

Dwivedi, N., Balomajumder, C. & Mondal, P. 2016 Comparative investigation on the removal of cyanide from aqueous solution using two different bioadsorbents. *Water Resources and Industry* **15**, 28–40. https://doi.org/10.1016/j.wri.2016.06.002.

Elkady, M. F., Ibrahim, A. M. & El-Latif, M. M. A. 2011 Assessment of the adsorption kinetics, equilibrium and thermodynamic for the potential removal of reactive Red dye using eggshell biocomposite beads. *Desalination* **278**(1–3), 412–423. https://doi.org/10.1016/j.desal.2011.05.063.

Fernandes, A., Iñiguez, A. M., Lima, V. S., De Souza, S. M. F. M., Ferreira, L. F., Vicente, A. C. P. & Jansen, A. M. 2008 Pre-Columbian Chagas Disease in Brazil: Trypanosoma Cruzi I in the archaeological remains of a human in Peruaçu Valley, Minas Gerais, Brazil. *Memorias Do Instituto Oswaldo Cruz* **103**(5), 514–516. https://doi.org/10.1590/S0074-02762008000500021.

Gulnaz, O., Sahmurova, A. & Kama, S. 2011 Removal of reactive Red 198 from aqueous solution by Potamogeton Crispus. *Chemical Engineering Journal* **174**(2–3), 579–585. https://doi.org/10.1016/j.cej.2011.09.061.

Guo, C., Ding, L., Jin, X., Zhang, H. & Zhang, D. 2021 Application of response surface methodology to optimize chromium (VI) removal from aqueous solution by cassava sludge-based activated carbon. *Journal of Environmental Chemical Engineering* **9**(1), 104785. https://doi.org/10.1016/j.jece.2020.104785.

Hammouda, I. & Mihoubi, D. 2014 Thermodynamic and mechanical characterisation of kaolin clay. *Polish Journal of Chemical Technology* **16**(1), 28–35. https://doi.org/10.2478/pjct-2014-0005.

Han, S., Zang, Y., Gao, Y., Yue, Q., Zhang, P., Kong, W., Jin, B., Xu, X. & Gao, B. 2020 Co-Monomer polymer anion exchange resin for removing Cr(VI) contaminants: adsorption kinetics, mechanism and performance. *Science of the Total Environment* **709**, 136002. https://doi.org/10.1016/j.scitotenv.2019.136002.

Harsha Hebbar, H. R., Math, M. C. & Yatish, K. V. 2018 Optimization and kinetic study of CaO nano-particles catalyzed biodiesel production from Bombax Ceiba oil. *Energy* **143**, 25–34. https://doi.org/10.1016/j.energy.2017.10.118.

Jjagwe, J., Wilberforce, P., Menya, E. & Mpagi, H. 2021 Synthesis and application of granular activated carbon from biomass waste materials for water treatment: a review. *Journal of Bioresources and Bioproducts* **6**(4), 292–322. https://doi.org/10.1016/j.jobab.2021.03.003.

Kassahun, E., Fito, J., Tibebu, S., Nkambule, T. T. I., Tadesse, T., Sime, T. & Kloos, H. 2022 The Application of the Activated Carbon from Cordia Africana Leaves for Adsorption of Chromium (III) from an Aqueous Solution. *Journal of Chemistry* **2022**, 11. https://doi.org/10.1155/2022/4874502.

Khosravi, R., Moussavi, G., Ghaneian, M. T., Ehrampoush, M. H., Barikbin, B., Ebrahimi, A. A. & Sharifzadeh, G. 2018 Chromium adsorption from aqueous solution using novel green nanocomposite: adsorbent characterization, isotherm, kinetic and thermodynamic investigation. *Journal of Molecular Liquids* **256**, 163–174. https://doi.org/10.1016/j.molliq.2018.02.033.

Koyachew, E. K. 2016 The problem of solid waste management and people awareness on appropriate solid waste disposal in Bahir Dar City: Amhara Region, Ethiopia. *ISABB Journal of Health and Environmental Sciences* **3**(1), 1–8. https://doi.org/10.5897/isaab-jhe2016.0026.

Kramarenko, V. V., Nikitenkov, A. N., Matveenko, I. A., Molokov, V. Y. & Vasilenko, Y. S. 2016 Determination of water content in clay and organic soil using microwave oven. *IOP Conference Series: Earth and Environmental Science* **43**(1). https://doi.org/10.1088/1755-1315/43/1/012029.

Kumar, V. V., Kumar, M. P., Thiruvenkadaravi, K. V., Baskaralingam, P., Kumar, P. S. & Sivanesan, S. 2012 Bioresource technology preparation and characterization of porous cross linked laccase aggregates for the decolorization of triphenyl methane and reactive dyes. *Bioresource Technology* **119**, 28–34. https://doi.org/10.1016/j.biortech.2012.05.078.

Kumar, S., Panda, A. K. & Singh, R. K. 2013 Preparation and characterization of acid and alkaline treated kaolin clay. *Bulletin of Chemical Reaction Engineering & Catalysis* **8**(1). https://doi.org/10.9767/bcrec.8.1.4530.61-69.

Liu, Q.-S., Zheng, T., Wang, P., Jiang, J.-P. & Li, N. 2010 Adsorption isotherm, kinetic and mechanism studies of some substituted phenols on activated carbon fibers. *Chemical Engineering Journal* **157**(2–3), 348–356. https://doi.org/10.1016/j.cej.2009.11.013.

Manoj, P., Reddy, K., Verma, P. & Subrahmanyam, C. 2015 Bio-waste derived adsorbent material for methylene blue adsorption. *Journal of the Taiwan Institute of Chemical Engineers*, 1–9. https://doi.org/10.1016/j.jtice.2015.07.006.

Matei, E., Maria, R., Covaliu, C. I., Negroiu, M. & Andreea Ţurcanu, A. 2021 Novel adsorbent based on banana peel waste for removal of heavy metal ions from synthetic solutions.

Mohan, D., Singh, K. P. & Singh, V. K. 2006 Trivalent chromium removal from wastewater using low cost activated carbon derived from agricultural waste material and activated carbon fabric cloth. *Journal of Hazardous Materials* **135**(1–3), 280–295. https://doi.org/10.1016/j.jhazmat.2005.11.075.

Negroiu, M., Ţurcanu, A. A., Matei, E., Râpă, M., Covaliu, C. I., Predescu, A. M., Pantilimon, C. M., Coman, G. & Predescu, C. 2021 Novel Adsorbent Based on Banana Peel Waste for Removal of Heavy Metal Ions from Synthetic Solutions. *Materials* **14**(14), 3946. https://doi.org/10.3390/ma14143946.

Naderi, M. 2015 Surface area: Brunauer – Emmett – Teller (BET). 585–608. https://doi.org/10.1016/B978-0-12-384746-1.00014-8.

Nahiun, K. M. 2021 A review on the methods of industrial waste water treatment. https://doi.org/10.32861/sr.73.20.31.

Padmavathy, K. S., Madhu, G. & Haseena, P. V. 2016 A study on effects of PH, adsorbent dosage, time, initial concentration and adsorption isotherm study for the removal of hexavalent chromium (Cr (VI)) from wastewater by magnetite nanoparticles. *Procedia Technology* **24**, 585–594. https://doi.org/10.1016/j.protcy.2016.05.127.

Palma, C., Contreras, E., Urra, J. & Martínez, M. J. 2011 Eco-friendly technologies based on banana peel use for the decolourization of the dyeing process wastewater. *Waste and Biomass Valorization* **2**(1), 77–86. https://doi.org/10.1007/s12649-010-9052-4.

Pathak, P. D., Mandavgane, S. A. & Kulkarni, B. D. 2016 Utilization of banana peel for the removal of benzoic and salicylic acid from aqueous solutions and its potential reuse. *Desalination and Water Treatment* **57**(27), 12717–12729. https://doi.org/10.1080/19443994.2015.1051589.

Ramutshatsha-makhwedzha, D., Mavhungu, A., Moropeng, M. L. & Mbaya, R. 2022 Heliyon activated carbon derived from waste orange and lemon peels for the adsorption of methyl orange and methylene blue dyes from wastewater. *Heliyon* **8**, e09930. https://doi.org/10.1016/j.heliyon.2022.e09930.

Saadatkhah, N., Garcia, A. C., Ackermann, S., Leclerc, P., Latifi, M., Samih, S., Patience, G. S. & Chaouki, J. 2020 Experimental methods in chemical engineering: thermogravimetric analysis – TGA. *Canadian Journal of Chemical Engineering* **98**(1), 34–43. https://doi.org/10.1002/cjce.23673.

Sadhukhan, B., Mondal, N. K. & Chattoraj, S. 2016 Optimisation using central composite design (CCD) and the desirability function for sorption of methylene blue from aqueous solution onto Lemna Major. *Karbala International Journal of Modern Science* **2**(3), 145–155. https://doi.org/10.1016/j.kijoms.2016.03.005.

Saini, R. D. 2017 Textile organic dyes: polluting effects and elimination methods from textile waste water. *International Journal of Chemical Engineering Research* **9**(1), 975–6442. Available from: http://www.ripublication.com.

Sarkar, S., Banerjee, A., Halder, U., Biswas, R. & Bandopadhyay, R. 2017 Degradation of synthetic Azo dyes of textile industry: a sustainable approach using microbial enzymes. *Water Conservation Science and Engineering* **2**(4), 121–131. https://doi.org/10.1007/s41101-017-0031-5.

Saruchi, P. & Kumar, V. 2019 Adsorption kinetics and isotherms for the removal of rhodamine B dye and Pb +2 ions from aqueous solutions by a hybrid ion-exchanger. *Arabian Journal of Chemistry* **12**(3), 316–329. https://doi.org/10.1016/j.arabjc.2016.11.009.

Sharma, S. & Bhattacharya, A. 2017 Drinking water contamination and treatment techniques. *Applied Water Science* **7**(3), 1043–1067. https://doi.org/10.1007/s13201-016-0455-7.

Shobier, A. H., El-sadaawy, M. M. & El-said, G. F. 2020 Removal of hexavalent chromium by ecofriendly raw marine Green Alga Ulva Fasciata: kinetic, thermodynamic and isotherm studies. *The Egyptian Journal of Aquatic Research* **46**(4), 325–331. https://doi.org/10.1016/j.ejar.2020.09.003.

Shuma, H. E., Mkayula, L. L. & Makame, Y. M. M. 2019 Assessment of the effect of acid activation of kaolin from malangali on water defluoridation. *Tanzania Journal of Science* **45**(1), 279–296.

Singh, K. & Arora, S. 2011 Removal of synthetic textile dyes from wastewaters: a critical review on present treatment technologies. *Critical Reviews in Environmental Science and Technology* **41**(9), 807–878. https://doi.org/10.1080/10643380903218376.

Sinto, J., Nugroho, Y. W. & Ilmi, H. 2018 *Preparation of Activated Carbon from Banana Peel Waste as Adsorbent for Preparation of Activated Carbon from Banana Peel Waste as Adsorbent for Motor Vehicle Exhaust Emissions*. https://doi.org/10.1051/e3sconf/20186703020.

Turki, A., Oudiani, A. E., Msahli, S. & Sakli, F. 2018 Infrared spectra for alfa fibers treated with thymol. *Journal of Glycobiology* **07**(01), 1–8. https://doi.org/10.4172/2168-958x.1000130.

Zamora-Ledezma, C., Negrete-Bolagay, D., Figueroa, F., Zamora-Ledezma, E., Ni, M., Alexis, F. & Guerrero, V. H. 2021 Heavy metal water pollution: a fresh look about hazards, novel and conventional remediation methods. *Environmental Technology and Innovation* **22**, 101504. https://doi.org/10.1016/j.eti.2021.101504.

Zhang, Y., Wang, Y., Zhang, H., Li, Y., Zhang, Z. & Zhang, W. 2020 Recycling spent lithium-ion battery as adsorbents to remove aqueous heavy metals: adsorption kinetics, isotherms, and regeneration assessment. *Resources, Conservation and Recycling* **156**, 104688. https://doi.org/10.1016/j.resconrec.2020.104688.

Zheng, W., Liu, Y., Liu, W., Ji, H., Li, F., Shen, C., Fang, X., Li, X. & Duan, X. 2021 A novel electrocatalytic filtration system with carbon nanotube supported nanoscale zerovalent copper toward ultrafast oxidation of organic pollutants. *Water Research* **194**, 116961. https://doi.org/10.1016/j.watres.2021.116961.

Ziarani, G. M., Moradi, R., Lashgari, N. & Kruger, H. G. 2018 Introduction and importance of synthetic organic dyes. *Metal-Free Synthetic Organic Dyes*, 1–7. https://doi.org/10.1016/b978-0-12-815647-6.00001-7.

First received 23 February 2023; accepted in revised form 11 March 2023. Available online 27 March 2023